PHYSICAL REVIEW B **93**, 081203(R) (2016)

Pure negatively charged state of the NV center in *n*-type diamond

Yuki Doi,[1] Takahiro Fukui,[1] Hiromitsu Kato,[2,3] Toshiharu Makino,[2,3] Satoshi Yamasaki,[2,3] Toshiyuki Tashima,[1] Hiroki Morishita,[1,4] Shinji Miwa,[1] Fedor Jelezko,[5] Yoshishige Suzuki,[1] and Norikazu Mizuochi[1,3,4,*]

[1]*Graduate School of Engineering Science, Osaka University, Toyonaka, Osaka 560-8531, Japan*

[2]*Energy Technology Research Institute, National Institute of Advanced Industrial Science and Technology (AIST), Tsukuba, Ibaraki 305-8568, Japan*

[3]*CREST, Japan Science and Technology Agency, Kawaguchi, Saitama 332-0012, Japan*

[4]*Institute for Chemical Research, Kyoto University, Gokasho, Uji-city, Kyoto 611-0011, Japan*

[5]*Institut für Quantenoptik, Universität Ulm, Albert-Einstein-Allee 11, 89081 Ulm, Germany*

(Received 8 December 2014; revised manuscript received 24 December 2015; published 3 February 2016)

Optical illumination on negatively charged nitrogen-vacancy (NV^-) centers inevitably causes stochastic charge-state transitions between the NV^- and the neutral charge state of the NV center. It limits the steady-state population of NV^- to 5% at minimum (∼610 nm) and 80% (∼532 nm) at maximum in intrinsic diamond depending on the wavelength. Here, we show Fermi-level control by phosphorus doping generates 99.4 ± 0.1% NV^- under 1-μW and 593-nm excitation which is close to maximum absorption of NV^-. The pure NV^- shows a fivefold increase in luminescence and a fourfold enhancement of an optically detected magnetic resonance under 593-nm excitation compared with those in intrinsic diamond.

DOI: 10.1103/PhysRevB.93.081203

Nitrogen-vacancy (NV) centers in diamond are the most promising candidates for various applications, such as quantum information science [1–8], magnetometry [9–13], and biosensing [14–16]. For these applications, controlling the charge state of the NV centers is crucial because optical initialization and readout of the spin state of the NV centers are only possible in a negatively charged one (NV^-). However, upon illumination, the NV centers undergo stochastic charge-state transitions between the NV^- and the neutral charge state of the NV center (NV^0) [17,18]. For example, upon excitation around 580 nm where NV^- has the highest absorption [17,19], NV^- easily turns into NV^0, and the steady-state population of NV^- decreases to about 10%, which could be revealed from single-shot charge-state measurements [17]. Therefore, illumination at 532 nm is usually used in the experiment for NV^-. This charge-state interconversion occurs upon illumination at any wavelength, so the steady-state NV^- population is always less than 75%–80% [17,20].

Generating a pure state including the charge state, close to 100% NV^- population, is very important for quantum information applications. Studies involving the preselection and reset of the charge state were carried out to achieve a high-fidelity operation because of the instability of the charge states [1,4,5]. However, this approach makes scaling up of diamond quantum registers more challenging. Furthermore, a single-shot readout of a nuclear spin indicates that the spin-flip probability of the conditional gate operation decreases because of the stochastic charge-state transitions [6,21]. In addition, such charge-state transitions lead to spectral diffusion [18,22,23] of the zero-phonon line of NV^-, which reduces the efficiency of two-photon quantum interference [4]. For nanoscale sensing applications, it is crucial to keep NV^- stable near the surface for high spatial resolution [15]; however, NV^- near the surface is unstable [24]. In addition, high-contrast fluorescence switching between pure bright NV^- and the pure dark state (NV^0) is also very important for super-resolution microscopy [25].

Previously, NV charge states were controlled by heavy neutron irradiation [26], surface termination [27–29], and combined optical and electrical operations [30–33]. Most of them were investigated by photoluminescence (PL) spectra, which only reveals a ratio of the charge states of the bright state. On the other hand, single-shot charge-state measurements can reveal population probability of NV^- and NV^0. Recently, deterministic control from NV^- to NV^0 by a purely electrical operation was revealed from the single-shot charge-state measurements [34]. Doping with nitrogen is considered to be one way to increase the NV^- population. Nitrogen donors (P1 centers) can donate electrons to NV^0, thereby changing its state to NV^- because the activation energy ($E_A = 1.70$ eV) of P1 is shallower than the acceptor level of the NV center [35], labeled (−/0) as shown in Fig. 1(a). However, the pure NV^- charge state, which can be revealed by the single-shot charge-state, has not yet been realized by nitrogen doping. Based on the activation energy, phosphorus is promising because that of phosphorus ($E_A = 0.57$ eV) [37] is much less than that of P1. Recently, charge states of ensemble NV centers were modulated by ion implantation of phosphorus and boron atoms [36]. However, population probability of the charge state is not shown. In the present study, we quantitatively investigate the charge-state population of single NV centers by using single-shot readout measurements in slightly phosphorus-doped *n*-type diamond synthesized by chemical vapor deposition (CVD). We obtain a pure NV^- population (>99% NV^-) and report its dynamics. It should be noted that, so far, *n*-type conductivity in diamond has only been realized by the CVD synthesis technique.

Phosphorus-doped *n*-type diamond samples were epitaxially grown by CVD onto Ib-type (111)-oriented diamond substrates with phosphorus concentrations of 5×10^{16} at cm^{-3} (sample A) and about 5×10^{15} at cm^{-3} (sample B) (see the Supplemental Material [38]). A homebuilt confocal microscope system was used to optically address single NV

*Corresponding author: mizuochi@scl.kyoto-u.ac.jp

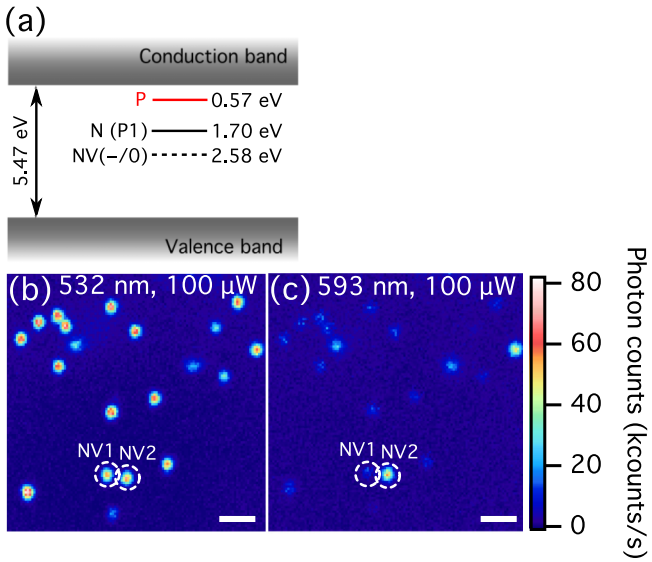

FIG. 1. (a) Donor energy levels of phosphorus (P) and nitrogen (P1) donors and acceptor level labeled (−/0) of the NV center with respect to conduction-band edge of diamond. (b) PL raster-scan images of single NV centers in n-type diamond (sample A, [P] = 5×10^{16} cm^{-3}) under 100-μW, 532-nm illumination. Most single NVs show similar optical properties under these illumination conditions. (c) The same as panel (b) but for 100-μW, 593-nm illumination. The fluorescence count rate of NV2 is about five times larger than that of NV1.

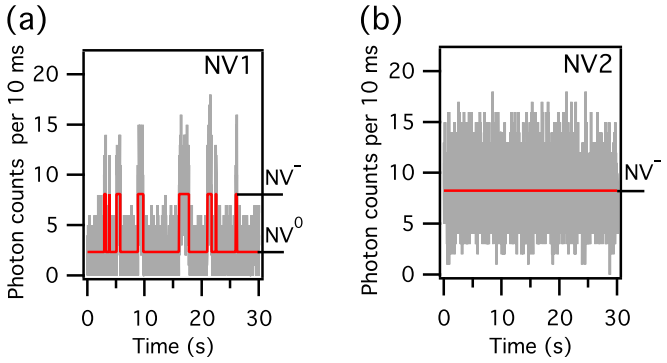

FIG. 2. (a) Time trace of the fluorescence of NV1 under continuous 1-μW, 593-nm illumination. Photon bursts occur when the charge state transforms into the NV$^-$ state. The solid red line shows the most probable fluorescence levels as obtained by the hidden Markov model. Here the average lifetimes of the two charge states are 2.92 s (NV^0) and 0.59 s (NV$^-$). (b) Time trace of the fluorescence of NV2 under the same illumination condition as for NV1. NV2 does not show photon bursts in the trace. The solid red line is the average count rate and is almost the same as the higher counts (NV$^-$) of NV1 in panel (a).

centers (see the Supplemental Material [38]). All experiments were conducted at room temperature.

No color centers other than single NV centers were detected in our high-quality samples under visible illumination. Typically, a high incorporation of nitrogen (such as more than 10^{15} at cm^{-3}) during CVD growth generates many NV centers. It makes it difficult to detect single NV centers. The fact that we detect many single NV centers in our samples reflects an advantage of phosphorus doping. Figures 1(b) and 1(c) show PL raster-scan images of n-type diamond (sample A) illuminated at 532 and 593 nm, respectively. Upon 532-nm illumination, the single NV center, labeled NV1, produces almost the same count rate (∼55 kcounts s^{-1}) as does the NV center labeled NV2. Upon 593-nm illumination, the counts rates of NV1 decrease because of the reduced NV$^-$ population as reported previously [17]. However, the counts rates from NV2 are about five times larger than that from NV1 (50 vs 10 kcounts s^{-1}). Moreover, in another area of samples A and B, more than ten single NV centers are bright under 593-nm illumination.

Weak excitation (typically 1 μW) at a 593-nm wavelength makes the charge-state interconversion of NV center gently. Thereby this is used for real-time detection of the charge states [17]. The charge states are distinguished by photon counts with optical filters (we used a 645-nm longpass filter) which blocks the fluorescence of NV^0. From the real-time fluorescence trace of NV1, shown in Fig. 2(a), the optically induced charge-state interconversion is recorded as telegraph signals of fluorescence from NV$^-$ (high counts) and NV^0 (low counts). In contrast to NV1, NV2 continuously keeps the fluorescence level of NV$^-$ [Fig. 2(b)]. These results suggest that NV2 populates to pure NV$^-$ under 1-μW, 593-nm illumination.

In order to observe charge-state population under 532- and 593-nm illumination, photon statistic measurements after illumination are performed. At NV1, the average lifetimes of NV^0 and NV$^-$ are 2.92 and 0.59 s, respectively, as determined by the hidden Markov model [17]. Therefore, for detection with 1-μW illumination at 593 nm, if the detection time is sufficiently less than 0.59 s, we can nondestructively determine charge-state population from the histogram of photon counts after arbitrary initialization (single-shot charge-state measurement). Figures 3(a) and 3(b) are measurement sequences and histograms of photon counts of NV1 after initialization by 30-μW, 532-nm and 1-μW, 593-nm illumination. For both initializations, the charge-state population of NV1 has a double Poisson distribution. For initialization at 532 nm, the charge-state populations are estimated to be NV^0 : NV$^-$ = 0.21 : 0.79 from the area of each peak. Upon initialization at 593 nm, NV$^-$ decreases to 0.12 on NV1 [Fig. 3(b)]. These populations are almost the same as single NV centers in intrinsic diamond [17]. In contrast to NV1, NV2 has only one peak on both sequences [Figs. 3(c) and 3(d)]. Peak widths and positions are quite similar to those of NV$^-$ in Fig. 3(a). This result strongly suggests that detected photons in single-shot measurements come from pure NV$^-$. The difference in the NV$^-$ population between NV1 and NV2 might be attributed to their different local environments (i.e., impurity and/or defects).

On the other hand, under 100-μW, 532-nm illumination, the PL spectrum and the optically detected magnetic resonance (ODMR) intensity of NV$^-$ on NV2 are the same as those of NV1 (see the Supplemental Material [38]). These results suggest that, under high power, 532-nm illumination, the charge-state population of NV2 is the same as that of NV1, despite a single peak being observed in Fig. 3(c). This fact implies that the charge state changes during the dark period (10 ms) between initialization and detection of the

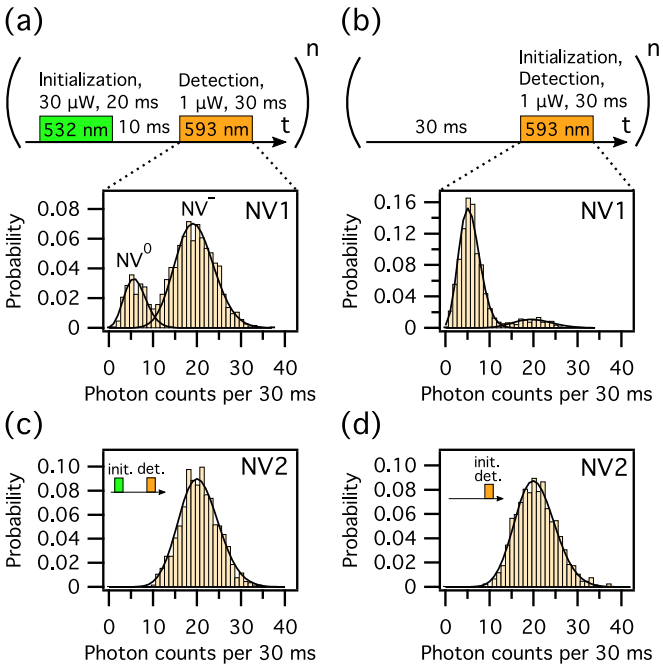

FIG. 3. Nondestructive single-shot charge-state measurements with two types of charge-state initialization: (a) 30-μW, 532-nm illumination and (b) 1-μW, 593-nm illumination. The NV1 population exhibits a double Poisson distribution that is due to two different charge states. Initialization at 593 nm drastically decreases the population of the NV^- charge state. (c) and (d) Conversely, NV2 has a single peak at the same position as NV^- irrespective of the initialization conditions. We repeated each sequence $n = 1000$ times for each histogram.

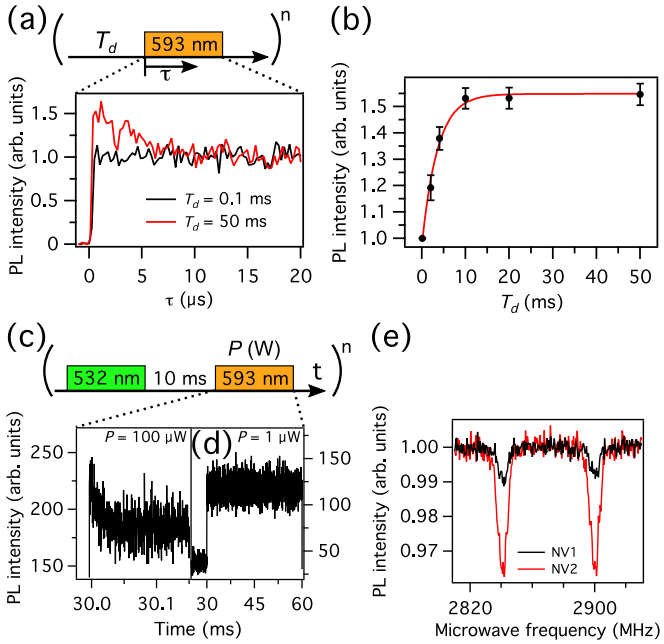

FIG. 4. (a) Increase in initial PL intensity of NV2 after time delay $T_d = 0.1$ and 50 ms under 230-μW and 593-nm illumination. PL intensity of NV2 increases after $T_d = 50$ ms. We repeated the sequence $n = 12\,209$ times. (b) PL intensity as a function of T_d. The fluorescence intensity is normalized to unity for $T_d = 0.1$ ms. The solid red line is a fit to a monoexponential with a time constant of 3.55 ms. (c) PL intensity for 593-nm illumination pulse $T_d = 10$ ms after initialization by the 532-nm illumination pulse. For 100-μW illumination, the PL intensity decays exponentially. (d) The same measurement as for panel (c) except the illumination was 1 μW, 593 nm. No decay in fluorescence intensity is observed. We repeated sequences $n = 17\,219$ and 9130 for $P = 100$ and 1-μW illumination, respectively. (e) ODMR spectrum of NV1 and NV2 under 200-μW 593-nm illumination. Signal intensity from NV^- of NV2 is almost 4.18 times larger than that from NV1. The amplitude of the applied magnetic field was 1 mT along the [111] direction of the diamond crystal.

single-shot charge-state measurements. To elucidate this fact, we average the PL intensity of NV2 after a time delay T_d. A 593-nm illumination with power of 230 μW is used to observe the decay of fluorescence. The measurement sequence and results are shown in Fig. 4(a). For $T_d = 0.1$ ms, the PL intensity does not change during illumination. This means the charge state of NV2 is in a state of equilibrium during T_d and illumination. However, when T_d increases to 50 ms, increases in intensity and exponential decay of PL are observed. The increase in intensity can be attributed to the increase in the NV^- population during the dark period (T_d). The subsequent decay is attributed to the decrease in the NV^- population during illumination by relatively higher power (230 μW) compared with 1 μW in the single-shot charge-state measurement.

To reveal the transition rate of the charge states during T_d, the PL intensity was measured as a function of T_d as shown in Fig. 4(b). The PL intensity clearly increases with T_d up to a saturation level. By fitting with a single exponential function, the transition rate from NV^0 to NV^- during T_d ($\lambda^{0-}_{\rm dark}$) is estimated to be $1/(3.55 \pm 0.42\,{\rm ms}) = 0.282 \pm 0.033\,{\rm ms}^{-1}$.

Next we investigate the dynamics during 593-nm illumination with several powers to show that the time constant for the charge-state transition is much longer than 30 ms under 1 μW, which is the power of the charge detection in Fig. 3. Figures 4(c) and 4(d) show the accumulated PL intensity of NV2 under 100- and 1-μW, 593-nm illumination after initialization by a 532-nm laser. The time delay T_d between the 532- and the 593-nm laser pulses was set at 10 ms, which is long enough for the NV^- population to grow to more than 99%. At 100-μW, 593-nm illumination, the PL intensity decays exponentially as shown in Fig. 4(c). This result indicates that the rate from NV^- to NV^0 by 593-nm illumination ($\lambda^{-0}_{593\,\rm nm}$) at 100 μW is greater than $\lambda^{0-}_{\rm dark} + \lambda^{0-}_{593\,\rm nm}$, where $\lambda^{0-}_{593\,\rm nm}$ is a rate from NV^0 to NV^- by 593-nm illumination. It was observed that the rate $\lambda^{0-}_{593\,\rm nm}$ and $\lambda^{-0}_{593\,\rm nm}$ becomes smaller as the laser power decreases. At 1-μW illumination, no decay in fluorescence intensity is observed as shown in Fig. 4(d). This also supports the fact that the charge state is at equilibrium and purely populated to NV^- under 1-μW, 593-nm illumination.

We quantitatively estimate the population of NV^- to use transition rates. Under 593-nm cw illumination, the steady-state-population of NV^- ($p_{\rm NV^-}$) can be calculated as follows [17,34]:

$$p_{\rm NV^-} = \frac{\lambda^{0-}}{\lambda^{0-} + \lambda^{-0}} = \frac{\lambda^{0-}_{593\,\rm nm} + \lambda^{0-}_{\rm dark}}{\lambda^{0-}_{593\,\rm nm} + \lambda^{0-}_{\rm dark} + \lambda^{-0}_{593\,\rm nm}}. \quad (1)$$

We omitted $\lambda^{-0}_{\mathrm{dark}}$ because it is negligibly smaller than the other rates [if it is not zero, the histograms of Figs. 2(c) and 2(d) must contain two Poisson distributions]. Here the optically induced transition rates ($\lambda^{0-}_{593\,\mathrm{nm}}$ and $\lambda^{-0}_{593\,\mathrm{nm}}$) for NV1 under 1-$\mu$W, 593-nm illumination can be obtained by average lifetimes of NV^0 and NV^- in Fig. 2(a). These rates are estimated to be $\lambda^{0-}_{593\,\mathrm{nm}} = 1/2.92\,\mathrm{s} = 0.342\,\mathrm{s}^{-1}$ and $\lambda^{-0}_{593\,\mathrm{nm}} = 1/0.59\,\mathrm{s} = 1.7\,\mathrm{s}^{-1}$. If these values of NV2 are assumed to be the same as those for NV1, $p_{\mathrm{NV^-}}$ for NV2 under 1-μW, 593-nm illumination is estimated to be $p_{\mathrm{NV^-}} = 0.994 \pm 0.001$ from Eq. (1). For reference, $p_{\mathrm{NV^-}}$ for NV1 is calculated to be 0.170 (where $\lambda^{0-}_{\mathrm{dark}} = 0$), which is consistent with the charge-state population in Fig. 3(b). The case for the 532-nm excitation can be analyzed, and it is indicated that a population consisting solely of the NV^- charge state can be generated by low-power 532-nm illumination (see the Supplemental Material [38]).

In NV2, we found a fourfold enhancement of an ODMR under 593-nm excitation compared with that of NV1. Figure 4(e) shows ODMR spectra of NV1 and NV2 with a 1-mT magnetic field along the [111] direction of the diamond crystal under 200-μW, 593-nm illumination. From NV2, the ODMR signal intensity from NV^-, which is the normalized fluorescence intensity, is almost 4.18 times larger than that from NV1. This result confirms that the NV^- population of NV2 is much larger than that of NV1 and single peaks in Figs. 3(c) and 3(d) are from the NV^- charge state. To measure the ODMR spectra, we increased the 593-nm laser power to 200 μW. At 200 μW, the charge state is not considered to be a purely negative state. Under 593-nm, 1-μW illumination, the ratio of NV^- population between NV2 and NV1 is calculated to be $100\%/12\% = 8.33$ from the results of Figs. 3(b) and 3(d). The enhanced ratio of the ODMR signal intensity (=4.18) is smaller than it. The main reason is considered to be due to the smaller ratio of NV^- population at the high laser power (200 μW). In our case, NV1 and NV2 are aligned with the [111] direction of the diamond crystal. Therefore, we assume the microwave power, the amplitude, and the polarization of the laser of NV2 are the same with those of NV1. In the general case where NVs feel different microwave powers, amplitudes, and polarizations of the laser from each other, we need to consider the effects of broadening of the spectra [39].

Finally, we measured spin-coherence time T_2 by the Hahn echo technique because a long T_2 is critical for quantum information and sensing. As a result, T_2 is estimated to be 19.77 ± 0.27 μs for NV2 in sample A ($[\mathrm{P}] = 5\times10^{16}\,\mathrm{cm}^{-3}$) and 49.6 ± 2.2 μs for sample B ($[\mathrm{P}] = 5\times10^{15}\,\mathrm{cm}^{-3}$) (see the Supplemental Material [38]). Previously, dependence of the nitrogen donors' (i.e., P1 centers) concentration on T_2 of the P1 centers was investigated, and T_2 of the P1 centers is estimated to be about 1 ms and 100 μs for the P1 concentration of 5×10^{15} and $5\times10^{16}\,\mathrm{cm}^{-3}$, respectively [40]. We expect the dependence of the phosphorus concentration on T_2 of the NV centers to be almost the same as that of the P1 center because the unpaired electrons localize on their atoms. However, the present results of T_2 are shorter than the expected values. It can be attributed to other impurities or defects [41]. In other words, if these impurities or defects could be removed and if ^{12}C could be enriched, T_2 in the n-type diamond should become comparable to the long (millisecond order) T_2 of high-quality intrinsic ^{12}C-enriched diamond [13,42].

To summarize, we investigated the NV^- population and its dynamics in phosphorus-doped n-type diamond by using nondestructive single-shot readout measurements of the NV charge state. In phosphorus-doped n-type diamond, the results reveal that the NV^- charge state that populates over 99% of the NV centers is generated by 1-μW illumination at 593 nm. Under these illumination conditions, we obtain an almost fivefold increase in luminescence and a fourfold increase in the ODMR signal compared with the corresponding results for the NV centers in intrinsic diamond. By analyzing the NV^- population as a function of illumination, we show that this approach would increase the NV^- population not only under 593-nm illumination, but also under illumination by other wavelengths, such as 532 nm. These results are expected to significantly enhance the versatile potential of NV centers.

This work was supported by JSPS KAKENHI Grant No. 15J05801. The authors gratefully acknowledge the financial support from NICT as well as from the JST CREST program. F.J. acknowledges DFG, EU, ERC, Volkswagenstiftung, and DARPA.

[1] G. Waldherr, Y. Wang, S. Zaiser, M. Jamali, T. Schulte-Herbrüggen, H. Abe, T. Ohshima, J. Isoya, J. F. Du, P. Neumann, and J. Wrachtrup, Quantum error correction in a solid-state hybrid spin register, Nature (London) **506**, 204 (2014).

[2] P. C. Maurer, G. Kucsko, C. Latta, L. Jiang, N. Y. Yao, S. D. Bennett, F. Pastawski, D. Hunger, N. Chisholm, M. Markham, D. J. Twitchen, J. I. Cirac, and M. D. Lukin, Room-temperature quantum bit memory exceeding one second, Science **336**, 1283 (2012).

[3] T. van der Sar, Z. H. Wang, M. S. Blok, H. Bernien, T. H. Taminiau, D. M. Toyli, D. A. Lidar, D. D. Awschalom, R. Hanson, and V. V. Dobrovitski, Decoherence-protected quantum gates for a hybrid solid-state spin register, Nature (London) **484**, 82 (2012).

[4] H. Bernien, B. Hensen, W. Pfaff, G. Koolstra, M. S. Blok, L. Robledo, T. H. Taminiau, M. Markham, D. J. Twitchen, L. Childress, and R. Hanson, Heralded entanglement between solid-state qubits separated by three metres, Nature (London) **497**, 86 (2013).

[5] L. Robledo, L. Childress, H. Bernien, B. Hensen, P. F. A. Alkemade, and R. Hanson, High-fidelity projective read-out of a solid-state spin quantum register, Nature (London) **477**, 574 (2011).

[6] P. Neumann, J. Beck, M. Steiner, F. Rempp, H. Fedder, P. R. Hemmer, J. Wrachtrup, and F. Jelezko, Single-shot readout of a single nuclear spin, Science **329**, 542 (2010).

[7] L. Childress, M. V. G. Dutt, J. M. Taylor, A. S. Zibrov, F. Jelezko, J. Wrachtrup, P. R. Hemmer, and M. D. Lukin,

Coherent dynamics of coupled electron and nuclear spin qubits in diamond, Science **314**, 281 (2006).

[8] V. Jacques, E. Wu, F. Grosshans, F. Treussart, P. Grangier, A. Aspect, and J.-F. Roch, Experimental realization of Wheeler's delayed-choice Gedanken experiment, Science **315**, 966 (2007).

[9] J. R. Maze, P. L. Stanwix, J. S. Hodges, S. Hong, J. M. Taylor, P. Cappellaro, L. Jiang, M. V. G. Dutt, E. Togan, A. S. Zibrov, A. Yacoby, R. L. Walsworth, and M. D. Lukin, Nanoscale magnetic sensing with an individual electronic spin in diamond, Nature (London) **455**, 644 (2008).

[10] G. Balasubramanian, I. Y. Chan, R. Kolesov, M. Al-Hmoud, J. Tisler, C. Shin, C. Kim, A. Wojcik, P. R. Hemmer, A. Krueger, T. Hanke, A. Leitenstorfer, R. Bratschitsch, F. Jelezko, and J. Wrachtrup, Nanoscale imaging magnetometry with diamond spins under ambient conditions, Nature (London) **455**, 648 (2008).

[11] H. J. Mamin, M. Kim, M. H. Sherwood, C. T. Rettner, K. Ohno, D. D. Awschalom, and D. Rugar, Nanoscale nuclear magnetic resonance with a nitrogen-vacancy spin sensor, Science **339**, 557 (2013).

[12] F. Shi, X. Kong, P. Wang, F. Kong, N. Zhao, R.-B. Liu, and J. Du, Sensing and atomic-scale structure analysis of single nuclear-spin clusters in diamond, Nat. Phys. **10**, 21 (2013).

[13] G. Balasubramanian, P. Neumann, D. J. Twitchen, M. Markham, R. Kolesov, N. Mizuochi, J. Isoya, J. Achard, J. Beck, J. Tissler, V. Jacques, P. R. Hemmer, F. Jelezko, and J. Wrachtrup, Ultralong spin coherence time in isotopically engineered diamond, Nat. Mater. **8**, 383 (2009).

[14] L. P. McGuinness, Y. Yan, A. Stacey, D. A. Simpson, L. T. Hall, D. Maclaurin, S. Prawer, P. Mulvaney, J. Wrachtrup, F. Caruso, R. E. Scholten, and L. C. L. Hollenberg, Quantum measurement and orientation tracking of fluorescent nanodiamonds inside living cells, Nat. Nanotechnol. **6**, 358 (2011).

[15] T. Staudacher, F. Shi, S. Pezzagna, J. Meijer, J. Du, C. A. Meriles, F. Reinhard, and J. Wrachtrup, Nuclear magnetic resonance spectroscopy on a (5-Nanometer)^3 sample volume, Science **339**, 561 (2013).

[16] D. Le Sage, K. Arai, D. R. Glenn, S. J. DeVience, L. M. Pham, L. Rahn-Lee, M. D. Lukin, A. Yacoby, A. Komeili, and R. L. Walsworth, Optical magnetic imaging of living cells, Nature (London) **496**, 486 (2013).

[17] N. Aslam, G. Waldherr, P. Neumann, F. Jelezko, and J. Wrachtrup, Photo-induced ionization dynamics of the nitrogen vacancy defect in diamond investigated by single-shot charge state detection, New J. Phys. **15**, 013064 (2013).

[18] P. Siyushev, H. Pinto, M. Vörös, A. Gali, F. Jelezko, and J. Wrachtrup, Optically Controlled Switching of the Charge State of a Single Nitrogen-Vacancy Center in Diamond at Cryogenic Temperatures, Phys. Rev. Lett. **110**, 167402 (2013).

[19] A. S. Trifonov, J. C. Jaskula, C. Teulon, D. R. Glenn, N. Bar-Gill, and R. L. Walsworth, Limits to resolution of CW STED microscopy, Adv. At., Mol., Opt. Phys. **62**, 279 (2013).

[20] X.-D. Chen, C.-L. Zou, F.-W. Sun, and G.-C. Guo, Optical manipulation of the charge state of nitrogen-vacancy center in diamond, Appl. Phys. Lett. **103**, 013112 (2013).

[21] G. Waldherr, J. Beck, M. Steiner, P. Neumann, A. Gali, T. Frauenheim, F. Jelezko, and J. Wrachtrup, Dark States of Single Nitrogen-Vacancy Centers in Diamond Unraveled by Single Shot NMR, Phys. Rev. Lett. **106**, 157601 (2011).

[22] A. Stacey, D. A. Simpson, T. J. Karle, B. C. Gibson, V. M. Acosta, Z. Huang, K.-M. C. Fu, C. Santori, R. G. Beausoleil, L. P. McGuinness, K. Ganesan, S. Tomljenovic-Hanic, A. D. Greentree, and S. Prawer, Near-Surface Spectrally Stable Nitrogen Vacancy Centres Engineered in Single Crystal Diamond, Adv. Mater. **24**, 3333 (2012).

[23] V. M. Acosta, C. Santori, A. Faraon, Z. Huang, K.-M. C. Fu, A. Stacey, D. A. Simpson, K. Ganesan, S. Tomljenovic-Hanic, A. D. Greentree, S. Prawer, and R. G. Beausoleil, Dynamic Stabilization of the Optical Resonances of Single Nitrogen-Vacancy Centers in Diamond, Phys. Rev. Lett. **108**, 206401 (2012).

[24] B. K. Ofori-Okai, S. Pezzagna, K. Chang, M. Loretz, R. Schirhagl, Y. Tao, B. A. Moores, K. Groot-Berning, J. Meijer, and C. L. Degen, Spin properties of very shallow nitrogen vacancy defects in diamond, Phys. Rev. B **86**, 081406 (2012).

[25] K. Y. Y. Han, S. K. Kim, C. Eggeling, and S. W. Hell, Metastable Dark states enable ground state depletion microscopy of nitrogen vacancy centers in diamond with diffraction-unlimited resolution, Nano Lett. **10**, 3199 (2010).

[26] Y. Mita, Change of absorption spectra in type-Ib diamond with heavy neutron irradiation, Phys. Rev. B **53**, 11360 (1996).

[27] C. Bradac, T. Gaebel, N. Naidoo, M. J. Sellars, J. Twamley, L. J. Brown, A. S. Barnard, T. Plakhotnik, A. V. Zvyagin, and J. R. Rabeau, Observation and control of blinking nitrogen-vacancy centres in discrete nanodiamonds, Nat. Nanotechnol. **5**, 345 (2010).

[28] M. V. Hauf, B. Grotz, B. Naydenov, M. Dankerl, S. Pezzagna, J. Meijer, F. Jelezko, J. Wrachtrup, M. Stutzmann, F. Reinhard, and J. A. Garrido, Chemical control of the charge state of nitrogen-vacancy centers in diamond, Phys. Rev. B **83**, 081304 (2011).

[29] T. W. Shanley, A. A. Martin, I. Aharonovich, and M. Toth, Localized chemical switching of the charge state of nitrogen-vacancy luminescence centers in diamond, Appl. Phys. Lett. **105**, 063103 (2014).

[30] N. Mizuochi, T. Makino, H. Kato, D. Takeuchi, M. Ogura, H. Okushi, M. Nothaft, P. Neumann, A. Gali, F. Jelezko, J. Wrachtrup, and S. Yamasaki, Electrically driven single-photon source at room temperature in diamond, Nat. Photon. **6**, 299 (2012).

[31] B. Grotz, M. V. Hauf, M. Dankerl, B. Naydenov, S. Pezzagna, J. Meijer, F. Jelezko, J. Wrachtrup, M. Stutzmann, F. Reinhard, and J. A. Garrido, Charge state manipulation of qubits in diamond, Nat. Commun. **3**, 729 (2012).

[32] H. Kato, M. Wolfer, C. Schreyvogel, M. Kunzer, W. Müller-Sebert, H. Obloh, S. Yamasaki, and C. Nebel, Tunable light emission from nitrogen-vacancy centers in single crystal diamond PIN diodes, Appl. Phys. Lett. **102**, 151101 (2013).

[33] M. V. Hauf, P. Simon, N. Aslam, M. Pfender, P. Neumann, S. Pezzagna, J. Meijer, J. Wrachtrup, M. Stutzmann, F. Reinhard, and J. A. Garrido, Addressing Single Nitrogen-Vacancy Centers in Diamond with Transparent in-Plane Gate Structures, Nano Lett. **14**, 2359 (2014).

[34] Y. Doi, T. Makino, H. Kato, D. Takeuchi, M. Ogura, H. Okushi, H. Morishita, T. Tashima, S. Miwa, S. Yamasaki, P. Neumann, J. Wrachtrup, Y. Suzuki, and N. Mizuochi, Deterministic Electrical Charge-State Initialization of Single Nitrogen-Vacancy Center in Diamond, Phys. Rev. X **4**, 011057 (2014).

[35] J. P. Goss, P. R. Briddon, R. Jones, and S. Sque, Donor and acceptor states in diamond, Diam. Relat. Mater. **13**, 684 (2004).

[36] K. Groot-Berning, N. Raatz, I. Dobrinets, M. Lesik, P. Spinicelli, A. Tallaire, J. Achard, V. Jacques, J.-F. Roch, A. M. Zaitsev, J. Meijer, and S. Pezzagna, Passive charge state control of nitrogen-vacancy centres in diamond using phosphorous and boron doping, Phys. Status Solidi A **211**, 2268 (2014).

[37] M. Katagiri, J. Isoya, S. Koizumi, and H. Kanda, Lightly phosphorus-doped homoepitaxial diamond films grown by chemical vapor deposition, Appl. Phys. Lett. **85**, 6365 (2004).

[38] See Supplemental Material at http://link.aps.org/supplemental/10.1103/PhysRevB.93.081203 for details of the experiments.

[39] A. Dréau, M. Lesik, L. Rondin, P. Spinicelli, O. Arcizet, J.-F. Roch, and V. Jacques, Avoiding power broadening in optically detected magnetic resonance of single NV defects for enhanced dc magnetic field sensitivity, Phys. Rev. B **84**, 195204 (2011).

[40] J. A. van Wyk, E. C. Reynhardt, G. L. High, and I. Kiflawi, The dependences of ESR line widths and spin-spin relaxation times of single nitrogen defects on the concentration of nitrogen defects in diamond, J. Phys. D: Appl. Phys. **30**, 1790 (1997).

[41] N. Mizuochi, H. Watanabe, J. Isoya, H. Okushi, and S. Yamasaki, Hydrogen-related defects in single crystalline CVD homoepitaxial diamond film studied by EPR, Diam. Relat. Mater. **13**, 765 (2004).

[42] N. Mizuochi, P. Neumann, F. Rempp, J. Beck, V. Jacques, P. Siyushev, K. Nakamura, D. J. Twitchen, H. Watanabe, S. Yamasaki, F. Jelezko, and J. Wrachtrup, Coherence of single spins coupled to a nuclear spin bath of varying density, Phys. Rev. B **80**, 041201 (2009).